Pol. J. Environ. Stud. Vol. 26, No. 6 (2017), 2777-2783
DOI: *10.15244/pjoes/70442* ONLINE PUBLICATION DATE: 2017-10-31

Original Research

Photocatalytic Activity of $Al_2O_3.Fe_2O_3$ Synthesized by Ultrasonic-Assisted Mechanical Stirring

Inam Ullah[1]*, Shaukat Ali[1], Muhammad Asif Hanif[1], Muhammad Anjum Zia[2]

[1]Department of Chemistry, University of Agriculture, Faisalabad 38040, Pakistan
[2]Department of Biochemistry, University of Agriculture, Faisalabad 38040, Pakistan

Received: 22 January 2017
Accepted: 12 April 2017

Abstract

Water pollution has been a prime concern for scientists for decades. Different treatment methods have been suggested by different researchers, with photocatalysis emerging as an efficient method for treating industrial textile wastewater. This study is designed to synthesize a nano-photocatalyst for the degradation of two synthetic dyes. The $Al_2O_3.Fe_2O_3$ nano-photocatalyst was synthesized by a novel technique: ultrasonic-assisted mechanical stirring and synthesized photocatalyst characterized by x-ray diffraction (XRD), scanning electron microscopy (SEM), energy-dispersive x-ray (EDX) analysis, dynamic light scattering, and BET surface area analysis. The $Al_2O_3.Fe_2O_3$ nano-photocatalyst was tested for its potential to degrade methyl orange and methylene blue dyes. Important influencing parameters (pH, catalyst dose, initial dye concentration, and reaction time) have been optimized during the dye degradation process. The highest degradation for methyl orange (39%) and methylene blue (45%) was achieved by using 60 mg/100 mL catalyst dose and 120 minutes of reaction time at room temperature. The study results indicated that $Al_2O_3.Fe_2O_3$ nano-photocatalyst has good potential for the removal of dyes from industrial effluents.

Keywords: nano-photocatalyst, ultrasonic-assisted mechanical stirring technique, x-ray diffraction (XRD), scanning electron microscopy (SEM), energy-dispersive x-ray (EDX) analysis

Introduction

Water pollution is the burning issue of today's society and extensive research has been conducted in the field of wastewater treatment [1]. In countries like Pakistan, where the textile sector is playing a major role in the economy of the country, the textile industries are also responsible for enhancing the wastewater problem. Most textile industries release wastewater to the environment without any treatment [2-3]. Color is the major contaminant in textile effluents. The molecular structure of any contaminant provides good insight and helps formulate an effective treatment method for its removal from water streams. Most of the synthetic dyes (up to 70%) include azo group, which contains N = N bond in its molecular structure [4-5]. These synthetic dyes have complex aromatic

*e-mail: inam.ullah@yahoo.com
inam.ullah@hotmail.com

structures and a very efficient method is required for their removal from water bodies [6].

Different treatment technologies have been suggested by different researchers. Overall, the treatment methods can be categorized into physical methods, chemical methods, biological methods, and physico-chemical processes [7]. Physical methods don't degrade the structure of dyes but only change the phase [8]. Biological methods don't have the potential to degrade such a complex aromatic structure of synthetic dyes and are proved to be inefficient in this regard. In this context, the advanced oxidation processes that come under the category of chemical methods have been proved very efficient for destroying the synthetic dyes and this process does not require any critical conditions of temperature and pressure.

The concept of photocatalysis was proposed by Fujisheema and Honda in 1972, in which they proposed a method of conversion of solar energy into electrical energy [9]. Most of the study results indicate that photo catalysts can efficiently work at ambient temperature and pressure conditions, which makes the process more attractive [10-12]. The researchers are working hard on the development of efficient photocatalysts. The factors that significantly affect the photocatalytic activity of catalysts include size and morphology. Researchers are working on the synthesis of nano-photocatalysts by using different techniques, which include ball milling [13], arc spark methods [14], hydrothermal synthesis [15], electrochemical processes [16], reverse micelle reactions [17], chemical synthesis [18], and chemical co-precipitation [19]. Among these different methods, chemical co-precipitation has been found to be an efficient and low-cost technique [20].

The present study is designed to evaluate the photocatalytic efficiency of $Al_2O_3.Fe_2O_3$ nano-photocatalyst synthesized by ultrasonic-assisted mechanical stirring technique for the degradation of synthetic solutions of methyl orange (C.I. 13025) and methylene blue (C.I. 52015) dyes. Methyl orange is anionic in nature while methylene blue is a cationic dye. The synthesized nano-photocatalyst was characterized by XRD, EDX, and SEM, and its efficiency was checked for the degradation of synthetic dyes.

Materials and Method

Chemicals

All chemicals were of analytical grade and supplied from Sigma-Aldrich (USA) and Merck (Germany). MilliQ water was used throughout the experimental work.

Synthesis of $Al_2O_3.Fe_2O_3$ Nano-Photocatalyst

A co-precipitation technique was used to synthesize $Al_2O_3.Fe_2O_3$ nano-photocatalysts by a process reported by Shahid et al., 2010 [20]. A mechanical stirrer (IKA RW 20 Digital) was fit to a three-neck (Pyrex) flask of 500 mL capacity. A digital laboratory thermometer (Thermoprobe TL1W) was fit to one neck of the flask and a burette (Pyrex) was fit to the other neck for drop-wise addition of NH_3 solution. For the ultrasonic-assisted mechanical stirring co-precipitation method the flask was placed in an ultrasonic bath (Unisonics FXP12MH) where mechanical stirring and sonication were applied at the same time. Appropriate amounts of $AlCl_3$ and $FeCl_3.6H_2O$ were weighed and dissolved in 100 mL of deionized water separately at 65°C. The solutions were mixed and stirred at 500 rpm mechanically for 30 min at 65ºC, and then 30% NH_3 solution was added to the mixture solution drop-wise over 120 min to raise the pH of the slurry to 10 with constant stirring. The resulting reddish brown slurry was left stirring for another 60 min. The precipitates were centrifuged at 4,000 rpm, washed with deionized water, and finally washed with ethanol. The precipitates were separated and dried at 100ºC for 24 h in an oven. Dried samples were ground using an agate mortar and pestle to a fine powder and divided in three portions, and two of them were calcined at either 400 or 600ºC for 4 h in a muffle furnace. Samples were stored in air-sealed glass bottles for further use.

Characterization of $Al_2O_3.Fe_2O_3$

The crystalline phase and crystallite size of the nano-particles was determined by x-ray diffraction (XRD, Bruker D8 Advance) employing Cu Kα radiation (λ= 1.5406 Å, 2θ = 10 – 100º). XRD patterns of the samples were analyzed with the help of Match! 3.0.0 (phase identification software from powder diffraction) by Crystal Impact Bonn, Germany. We used the Crystallography Open Database (COD) REV129424 2015.01.07 for analysis. The crystallite size was determined using the Scherrer equation. The particle size was determined using a Zetasizer (Malvern Nano ZS). The morphology and elemental composition was determined by a scanning electron microscope (SEM, Philips XL 30) equipped with an energy-dispersive x-ray detector. The sample in minute quantity was sprinkled on the adhesive surface of magnetic tape and the tape was fixed on an aluminum stub and the stub sputter coated with Pt (Quorum Q150T). BET surface area and pore size of the samples were studied by N_2 adsorption desorption experiments on a Micromeritics Tristar 3000, where the samples were degassed at 150ºC for 12 h prior to measurement.

Photocatalytic Activity Evaluation

Methyl orange and methylene blue dyes were used as test pollutants. Degradation experiments were carried out by using a specific amount of photocatalyst mixed with 100 mL of dye solution (50 ppm), stirred for 30 min in the dark to equilibrate the adsorption-desorption process, and then the suspension was illuminated by visible light using a tungsten-halogen lamp. For the initial dye concentration experiment, the dye concentration for both the dyes varied from 20-60 ppm. Aliquots of 3 mL were removed and the

absorbance of Methyl Orange and Methylene blue was measured at 464 nm and 661 nm, respectively, by using a UV/Vis spectrophotometer (Schimadzu, Japan). A series of studies were carried out to evaluate the effect of pH, catalyst dose, initial dye concentration, and reaction time on the dye degradation process.

Kinetic Study

In the wastewater treatment process it is important to have a clear picture of the potential rate-controlling step of the process. For the degradation of dyes, the dye molecules first get adsorbed on the surface of the photocatalyst and then the catalyst degrades the dye molecules. Several kinetic models are available to describe adsorption kinetics. Most used models are pseudo first- and pseudo second-order. The applicability of these kinetic models was determined by measuring the correlation coefficients (R^2).

Results and Discussion

Characterization of $Al_2O_3.Fe_2O_3$

XRD Analysis of $Al_2O_3.Fe_2O_3$

The XRD pattern of $Al_2O_3.Fe_2O_3$ synthesized by ultrasonic-assisted mechanically stirred and calcined at 600°C are shown in Fig. 1a. Two types of crystal system were detected as basic sharp peaks at 2θ = 24.26°, 33.31°, 35.76°, 43.72°, 54.87°, 62.75°, 64.94°, 72.36°, 81.83°, 83.41°, and 89.04°, representing the α-Fe_2O_3 (Hematite) with trigonal crystal system according to entry number 96-901-4881. The gahnite phase was also detected at 2θ = 39.41°, 49.71°, 56.31°, 69.93°, 75.44°, and 94.29°, which are reported peaks for Al_2O_4Zn with cubic crystal system according to the entry number 96-900-7028.

Scanning Electron Microscopy of $Al_2O_3.Fe_2O_3$

A SEM image of the $Al_2O_3.Fe_2O_3$ synthesized by ultrasonic-assisted mechanically stirred co-precipitation is shown in Fig. 1b (Calcined at 600°C), and it is clear from the image that the photocatalyst has no specific shape.

Energy-Dispersive x-ray (EDX) Analysis of $Al_2O_3.Fe_2O_3$

EDX analysis of $Al_2O_3.Fe_2O_3$ synthesized by ultrasonic-assisted stirring during co-precipitation was performed with help of Philips XL 30 equipped with an EDX detector, and back scatter electron images of the samples were taken to analyze the chemical composition of the sample for qualitative and some estimation of molar and weight percentage of elements present in the sample. $Al_2O_3.Fe_2O_3$ is non-homogeneous material as its surface has different shades, and it looks like a pourous material at the same time. Spectra have very clear peaks for Fe, Al, and O, and a small peak of C also was observed, which is due to the magnetic tape used for supporting the sample on a stub (this peak was eliminated for weight and molar

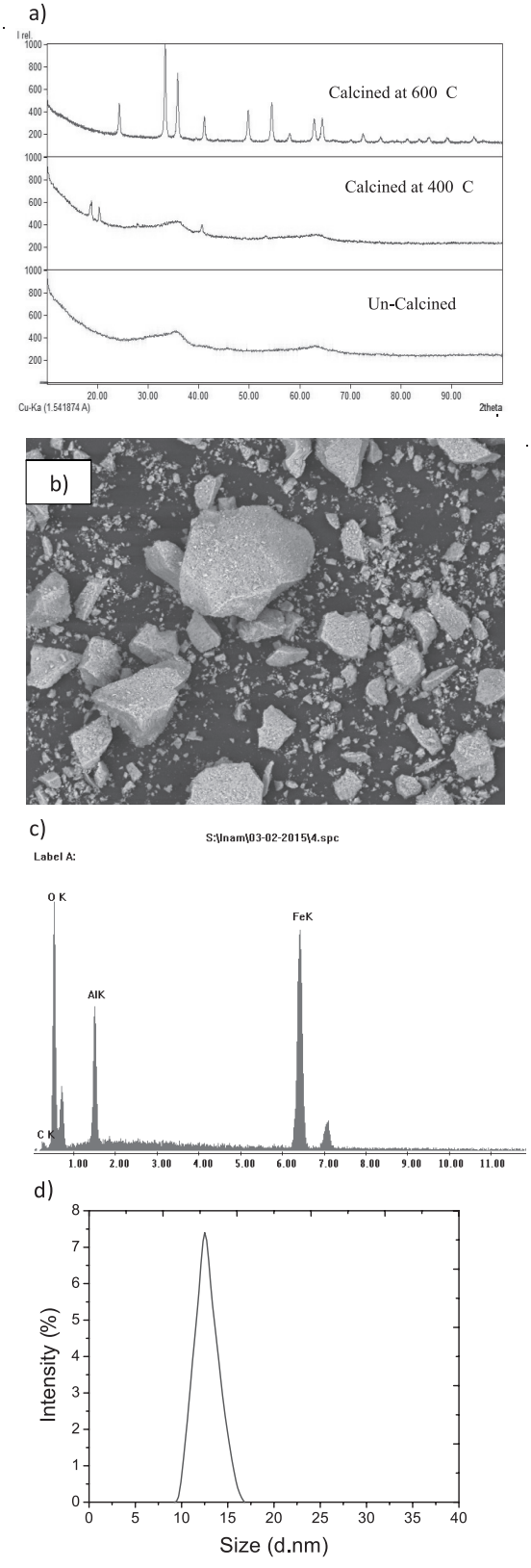

Fig. 1. Characterization of $Al_2O_3.Fe_2O_3$ nano-photocatalyst: a) XRD pattern, b) SEM image, c) EDX spectra, and d) particle size distribution.

percentage analysis; Fig. 1c). Estimated weights of Al_2O_3 and Fe_2O_3 from the EDX spectra are 22.74 and 77.26%, and the molar percentages of Al_2O_3 and Fe_2O_3 are 31.55 and 68.45%, respectively.

Particle Size, Surface Area, and Porosity Analysis

Particle size was analyzed by a Malvern Zetasizer (Nano ZS). Average particle size for Al_2O_3.Fe_2O_3 synthesized by ultrasonic-assisted mechanically stirred co-precipitation was 12.51 nm with Zetasizer, and by using Sherer's formula it was 11.09 nm. We observed from SEM images that particles were not of a specific shape so the Zetasizer calculates the diameter of particles from different directions and gives average particle size as distribution of particle size by intensity (Fig. 1d). Particle size was also calculated from x-ray diffraction patterns by using Scherer's formula. Both results have values close to each other with the confirmation of actual particle sizes. The effect of ultrasonic assisted stirring during co-precipitation is the decrease in particle sizes. Photocatalytic activity was improved due to small particle size and large surface area.

Photocatalytic Activity

We investigated the photocatalytic activity of Al_2O_3.Fe_2O_3 nano-photocatalyst for the degradation of the two synthetic dyes methyl orange and methylene blue. The study was conducted to evaluate the effect of pH, catalyst dose, and initial dye concentration and reaction time on the degradation of the two dyes.

Effect of pH

pH plays a very significant role in the dye degradation process. To evaluate the effect of pH on the degradation of methyl orange (MO) and methylene blue (MB) dyes, solution pH was varied from 1-9. The response of Al_2O_3.Fe_2O_3 nano-photocatalyst for degradation of both dyes was different by varying the solution pH (Fig. 2a). Maximum MO degradation (20.2%) was observed at pH 3 while maximum MB degradation (18.9 %) was achieved at pH 9. The reason behind this behavior is that MB is a cationic dye that was attracted toward negatively charged photocatalyst at high pH value. Due to this attraction, more dye molecules were adsorbed on the catalyst surface and photocatalytic activity was increased at higher pH [21]. Another factor that plays an important role is the availability of hydroxyl ions at high pH value. More hydroxyl ions were produced at higher pH, which leads to an increase in the production of OH radicals, which in turn increased oxidative degradation of MB at pH = 9 [22-24]. For MO, degradation efficiency was increased from pH 1 to 3 and then decreased from pH 3 to 9. Photocatalytic activity should be increased with the increase in pH as at higher pH values because more OH ions are available, which increases the formation of OH radicals [25]. But

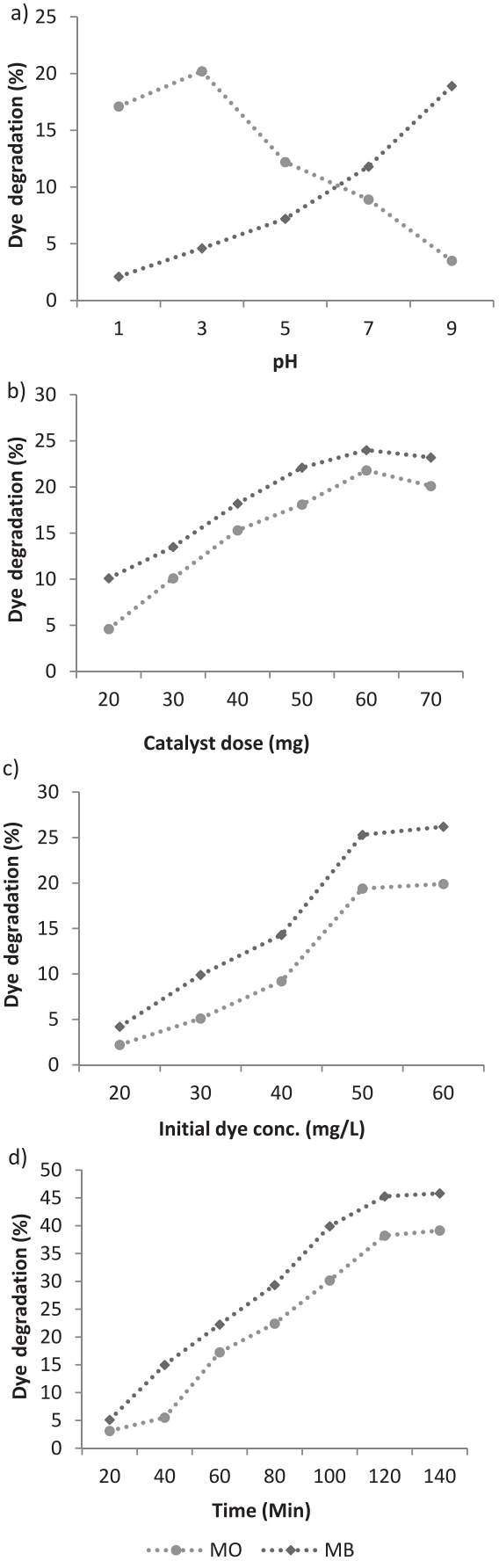

Fig. 2. Dependence of a) pH, b) catalyst dose, c) initial dye concentration, and d) reaction time on the percentage degradation of MO and MB dyes by Al_2O_3.Fe_2O_3 nano-photocatalyst.

in this case, different behavior was observed because at lower pH values the formation of HO_2 radicals takes place, which compensates for the deficiency of hydroxyl ions [26]. MO is anionic in nature and an oxidative attack of the hole on dye molecule is a rate-determining step, so at low pH this attack will be supported and more dye molecules will be degraded [27].

Effect of Catalyst Dose

The experiments were conducted to observe the effect of catalyst amount on the degradation of both dyes. For this purpose, the amount of Al_2O_3.Fe_2O_3 catalyst was varied from 20 mg to 70 mg/100 mL and results are shown in Fig. 2b). The experiment was performed at optimum pH for both dyes. The figure shows that dye degradation increased with increases in the catalyst dose from 20 mg to 60 mg. Maximum dye degradation for MO was found to be 21.8% and for MB it was 24%. When the Al_2O_3.Fe_2O_3 catalyst amount was increased further, a slight decrease in dye degradation efficiency of catalyst was observed. The increase in photocatalytic efficiency was due to the increase in the amount of nanophotocatalyst particles in the reaction mixture, which results in increased adsorption of dye molecules. The decrease in dye degradation efficiency at higher amounts is due to light scattering by accessing the amount of solid particles present in the reaction mixture [28-29]. Hence 60 mg/100 mL was found to be the optimum catalyst dose for both dyes.

Effect of Initial Dye Concentration

The initial concentration of dye in the solution is also a major contributing factor that can influence the catalytic activity of a photocatalyst. To evaluate this effect, the experiment was conducted by varying the initial dye concentration of both the dyes from 20 to 60 ppm. The experiment was conducted at optimum Al_2O_3.Fe_2O_3 catalyst dose and pH for one hour of reaction time. The results are shown in Fig. 2c), which shows that by increasing the initial dye concentration there was a remarkable increase in the percentage of dye degradation for both dyes. Maximum dye degradation was achieved at 50 ppm dye concentration for both the dyes (MB and MO). This is due to the fact that by increasing the number of dye molecules in solution, more dye molecules were available for adsorbing the active sites of the photocatalyst so the effective collisions were increased, which enhanced dye degradation. But further increases in initial concentration decreased the degradation efficiency of the photocatalyst due to decreases in intensity of light needed for the active photocatalyst [30]. This is due to the opacity of the reaction mixture, which may decrease the penetration of visible light in the reaction mixture [31].

Effect of Contact Time

Reaction time is a very important parameter to be optimized during the evaluation of any reaction. For optimization of this important parameter, the reaction time was varied from 20 minutes to 140 minutes and results can be seen in Fig. 2d). The results indicated that with the increase in reaction time, there was an increase in percentage dye degradation for both dyes. Maximum dye degradation for MO was 39% and for MB it was 45%. This was observed at 120 min of reaction time for both dyes. Further increase in time did not show any remarkable change in dye degradation. This is due to the fact that at the start on reaction more active sites are available to the dye molecules. With the progress of reaction the number of active sites available on the catalyst surface decreases and no more active sites become available for reaction, and the reaction mixture becomes stable.

Kinetic Studies

Pseudo first- and pseudo second-order kinetic models are applied on the experimental data to determine the major rate-controlling step.

The pseudo first-order kinetic model is based on the fact that the change in dye concentration with respect to time is proportional to power one. The integral form of the pseudo first-order model generally is expressed as:

$$\log(q_e - q_t) = \log q_e - K_1 . \frac{t}{2.303} \quad (1)$$

…where q_e and q_t are the adsorption capacity (mg/g) at equilibrium and time t, respectively; k_1 is the rate constant (L/min); and t is the contact time (min). According to the Lagergren pseudo first-order model, a plot of $\log(q_e - q_t)$ versus t gives a straight line with very poor correlation coefficient (R^2). Generally, the pseudo first-order kinetic model is found to be good only for the preliminary stage of the adsorption process. It is usually not fitted well for the whole data range of contact [32].

To understand the mechanism of adsorption over a complete range of contact time, the pseudo second-order kinetic model can be successfully applied. It can be expressed as:

$$\left(\frac{t}{q_t}\right) = \frac{1}{K_2 qe^2} + \frac{t}{qe} \quad (2)$$

…where K_2 (g/mg min) is the second order rate constant of the adsorption process.

A plot between t/q_t versus t gives the value of the constants K_2 (g/mg h), and q_e (mg/g) also can be calculated. The values of correlation coefficient (R^2) are very higher for both dyes. So the pseudo second-order kinetic model shows best fitness to the kinetic data and it is more appropriate and effective than the pseudo first-order kinetic model. These results are in agreement with the reported results of other researchers [33].

Conclusion

The study was designed to synthesize $Al_2O_3.Fe_2O_3$ nano-photocatalyst by an efficient technique; ultrasonic-assisted mechanical stirring. The synthesized catalyst was characterized by using different techniques, and study results indicate that this technique is very efficient for synthesis of small particle size material. The synthesized catalyst was tested for the degradation of methyl orange and methylene blue dyes. The maximum degradation achieved for methyl orange was 39% and for methylene blue it was found to be 45%.

Acknowledgements

The authors are thankful to the Higher Education Commission of Pakistan for financial assistance under the International Research Support Initiative Program (IRSIP), and the School of Chemistry and Molecular Biosciences, University of Queensland Australia for providing technical support. This work was carried out in part at the Centre for Microscopy and Microanalysis, the University of Queensland node of the Australian Microscopy and Microanalysis Research Facility (AMMRF).

References

1. SAHA P.D., CHOWDHURY S., MONDAL M., SINHA K. Biosorption of Direct Red 28 (Congo red) from aqueous solutions by eggshells: batch and column studies. Sep. Sci. Technol. **47**, 112, **2012**.
2. SADAF S., BHATTI H.N., NAUSHEEN S., AMIN M. Application of a novel lignocellulosic biomaterial for the removal of Direct Yellow 50 dye from aqueous solution: Batch and column study. J. Taiwan Inst. Chem. Eng. **47**, 160, **2015**.
3. AKAR T., ANILAN B., GORGULU A., AKAR S.T. Assessment of cationic dye biosorption characteristics of untreated and non-conventional biomass: pyracantha coccinea berries. J. Hazard. Mater. **168**, 1302, **2009**.
4. HSUEH C.L., HUANG Y.H., WANG C.C., CHEN C.Y. Degradation of azo dyes using low iron concentration of Fenton and Fenton-like system. Chemosphere. **58**, 1409, **2005**.
5. MITTAL A., GUPTA V.K., MALVIYA A., MITTAL J. Process development for the batch and bulk removal and recovery of a hazardous, water-soluble azo dye (Metanil Yellow) by adsorption over waste materials (bottom ash and de-oiled soya). J. Hazard. Mater. **151** (2–3), 821, **2008**.
6. MADHAVAN J., GRIESER F., ASHOKKUMAR M. Degradation of orange-G by advanced oxidation processes. Ultrason. Sonochem. **17**, 338, **2010**.
7. FORGACS E., CSERHATI T., OROS G. Removal of synthetic dyes from wastewaters: a review. Environ. Int. **30**, 953, **2004**.
8. JANUS M., MORAWSKI A.W. New method of improving photocatalytic activity of commercial Degussa P25 for azo dyes decomposition. Appl. Catal. B Environ. **75**, 118, **2007**.
9. MCMANAMON C., HOLMES J.D., MORRIS M.A. Improved photocatalytic degradation rates of phenol achieved using novel porous ZrO_2-doped TiO_2 nanoparticulate powders. J. Hazard Mater. **193**, 120, **2011**.
10. KARIMI L., ZOHOORI S., YAZDANSHENAS M.E. Photocatalytic degradation of azo dyes in aqueous solutions under UV irradiation using nano-strontium titanate as the nanophotocatalyst. J. Saudi Chem. Soc. **18**, 581, **2014**.
11. VINU R., AKKI S.U., MADRAS G. Investigation of dye functional group on the photocatalytic degradation of dyes by nano-TiO_2. J. Hazard. Mater. **176**, 765, **2010**.
12. CHEN C.Y. Photocatalytic degradation of azo dye reactive orange 16 by TiO_2. Water Air Soil Pollut. **202**, 335, **2009**.
13. TOKMAKCI T., ÖZTURK A., PARK J. Boron and zirconium co-doped TiO_2 powders prepared through mechanical ball milling. Ceramic Inter. **39**, 5893, **2013**.
14. ASHKARRAN A.A., AFSHAR S.A.A., AGHIGH S.M. Photocatalytic activity of ZrO_2 nanoparticles prepared by electrical arc discharge method in water. Polyhedron. **29**, 1370, **2010**.
15. GUAN B., WANG T., ZENG S., WANG X., AN D., WANG D., CAO Y., MA D., LIU Y., HUO Q. A versatile cooperative template-directed coating method to synthesize hollow and yolk-shell mesoporous zirconium titanium oxide nanospheres as catalytic reactors. Nano. Res. **7**, 246, **2014**.
16. JIANG W., HE J., ZHONG J., LU J., YUAN S., LIANG B. Preparation and photocatalytic performance of ZrO_2 nanotubes fabricated with anodization process. Appl. Surf. Sci. **307**, 407, **2014**.
17. GHIACI M., AGHAEI H., ABBASPUR A. Size-controlled synthesis of ZrO_2–TiO_2 nanoparticles prepared via reverse micelle method: investigation of particle size effect on the catalytic performance in vapor phase Beckmann rearrangement. Mater. Res. Bullet. **43**, 1255, **2008**.
18. RANI S., KUMAR M., SHARMA S., KUMAR D., TYAGI S. Effect of graphene in enhancing the photo catalytic activity of zirconium oxide. Catalysis letters. **144**, 301, **2014**.
19. ULLAH I., ALI S., HANIF M.A., ZIA M.A. Synthesis and Photocatalytic Efficiency of Sunlight Driven Novel Ternary Metal Oxide Nanophotocatalyst. Asian J. Chem. **27**, 1189, **2015**.
20. SHAHID M., SHAKIR I., YANG S.J., KANG D.J. Facile synthesis of core – shell SnO_2/V_2O_5 nanowires and their efficient photocatalytic property. Mater. Chem. Phy. **124**, 619, **2010**.
21. GUILLARD C., LACHHEB H., HOUAS A., KSIBI M., ELALOUI E., HERRMANN J.M. Influence of chemical structure of dyes, of pH and of inorganic salts on their photocatalytic degradation by TiO_2 comparison of the efficiency of powder and supported TiO_2. J. Photochem. Photobiol. A: Chem. **158** (1), **27**, **2003**.
22. CHAKRABARTI S., DUTTA B.K. Photocatalytic degradation of model textile dyes in wastewater using ZnO as semiconductor catalyst. J. Hazard. Mater. **112** (3), 269, **2004**.
23. TALEBIAN N., NILFOROUSHAN M. Comparative study of the structural, optical and photocatalytic properties of semiconductor metal oxides toward degradation of methylene blue. Thin Solid Films. **518** (8), 2210, **2010**.
24. SULTANA, S., KHAN M.Z., SHAHADAT M. Development of ZnO and ZrO_2 nanoparticles: Their photocatalytic and bactericidal activity. J. Environ. Chem. Eng. **3** (2), 886, **2015**.
25. KAUR J., BANSAL S., SINGHAL S. Photocatalytic degradation of methyl orange using ZnO nanopowders synthesized via thermal decomposition of oxalate precursor method. Physica B: Condensed Matter. **416**, 33, **2013**.

26. KU Y., HSIEH C.B. Photocatalytic decomposition of 2, 4-dichlorophenol in aqueous TiO_2 suspensions. Water research. **26** (11), 1451, **1992**.
27. Al-Qaradawi, S., Salman S.R. Photocatalytic degradation of methyl orange as a model compound. J. Photochem. Photobiol. A: Chem. **148** (1), 161, **2002**.
28. SARASIDIS V.C., PLAKAS K.V., PATSIOS S.I., KARABELAS A.J. Investigation of diclofenac degradation in a continuous photo-catalytic membrane reactor. Influence of operating parameters. Chem. Eng. J. **239**, 299, **2014**.
29. WANG X., ZHANG L., LIN H., NONG Q., WU Y., WU T., HE Y. Synthesis and characterization of a ZrO_2/gC_3N_4 composite with enhanced visible-light photoactivity for rhodamine degradation. RSC Adv. **4** (75), 40029, **2014**.
30. SHIRSATH S., PINJARI D., GOGATE P., SONAWANE S., PANDIT A. Ultrasound assisted synthesis of doped TiO_2 nano-particles: Characterization and comparison of effectiveness for photocatalytic oxidation of dyestuff effluent. Ultrasonic sonochem. **20** (1), 277, **2013**.
31. SWETHA S., BALAKRISHNA R.G. Preparation and characterization of high activity zirconium-doped anatase titania for solar photocatalytic degradation of ethidium bromide. Chinese J. Catal. **32** (5), 789, **2011**.
32. MCKAY G., HO Y.S. The sorption of lead(II) on peat. Water Res. **33**, 578, **1999**.
33. HAMEED B.H. Evaluation of papaya seeds as a novel non-conventional low-cost adsorbent for removal of methylene blue. J. Hazard. Mater. **162**, 939, **2009**.